Part I

Antimonide Related Materials — Growth, Characterization, and Analysis

MATERIALS FOR MID-INFRARED SEMICONDUCTOR LASERS

A. R. KOST
Hughes Research Laboratories, Malibu, CA 90265, arkost@hrl.com

ABSTRACT

A variety of semiconductor materials have been used to fabricate diode lasers for the mid-infrared. Lasers using the lead salts (e.g. PbSnTe) have been commercially available for some time. Mid-infrared emitting III-V semiconductors (e.g. InGaAsSb) have superior thermal conductivity, and diode lasers fabricated from these materials offer higher powers. Of particular interest are the III-V semiconductor lasers based on type-II superlattices (e.g. InAs/GaInSb). Among the many unique properties attributed to type-II superlattices are small hole mass, reduced Auger recombination, and less inter-valence band absorption - all important for better lasers. Recent results with Quantum Cascade-type lasers are also very encouraging. This paper summarizes the important semiconductor materials for mid-infrared lasers with emphasis on the type-II superlattices.

INTRODUCTION

Interest in diode lasers operating in the 2-5 μm (MID-IR) wavelength range is driven by applications in spectroscopy, trace gas sensing, and infrared counter measures. In many cases, diode lasers with high output power are desirable as are diode lasers that operate at or near room temperature but not necessarily both. Generally, application to spectroscopy or trace gas sensing requires low to moderate power and high operating temperature. For infrared counter measures, high power (~ 1 Watt) is most important. For all applications, device reliability is important.

Among the most promising devices are those that have been fabricated from III-V semiconductor alloys containing antimony [1-7]. In particular, it has been proposed that GaInSb/InAs type-II superlattices offer improved laser performance in the MID-IR as a result of reduced Auger recombination [8,9]. Here we survey the semiconductors for MID-IR lasers and summarize the work with type-II superlattices. Although most work on MID-IR semiconductor lasers has emphasized the development of improved active regions, it is important to note that it is not the way that lasers can be improved. Optical cladding layers with low electrical resistance are also important for good performance.

LEAD SALT MATERIALS

Semiconductors based on lead salts (e.g. PbSnTe for the active layer) have been commercially available for some time. They are characterized by relatively small Auger coefficients and a very broad range of operating wavelengths (~ 3 μm to ~ 30 μm). Perhaps the most impressive MID-IR lead salt laser was a PbSe-PbSrSe multiple quantum well (MQW) device that operated at 4.2 μm up to 282K under pulsed current injection [10]. The lead salt semiconductors have low thermal conductivity (~ 0.1 W/cm•K at 77K), and lead salt lasers have correspondingly small output power, on the order of 1 mW or less. All lead salt lasers operate below room temperature. Difficulty in growing high quality hetero-junctions with these materials translates into poor device reliability. Finally, lead salt technology is mature, so we don't expect big improvements in the performance of the lead salt lasers in the near future.

II-VI SEMICONDUCTORS

There has been relatively little work on lasers based on the II-VI semiconductors. Perhaps the lack of interest can be explained by modest device performance, e.g. pulsed operation of a 2.9 μm HgCdTe device at 90K [11], and problems which are also associated with the lead salt materials. Like the lead salts, the II-VI semiconductors have relatively small thermal

Mat. Res. Soc. Symp. Proc. Vol. 484 © 1998 Materials Research Society

conductivities, and high quality epitaxial growth is difficult.

III-V ALLOYS

In order to achieve good lattice matching, much of the MID-IR laser work with III-V semiconductors has concentrated on the GaInAsSb alloys (or the InAsSb subset) grown on InAs or GaSb substrates. The III-V alloys have good thermal conductivity, and lasers based on these materials have moderate output, e.g. 215 mW/facet cw at 3.5 μm for an InAsSb-AlInAsSb MQW device at 80K [12]. Like the lead salt and II-VI semiconductor lasers, MID-IR lasers employing III-V alloys operate below room temperature, e.g. maximum operating temperature of 175K for cw operation of the InAsSb-AlInAsSb MQW device [12]. Recently, a differential efficiency of 90% was reported for an InAsSbP-InAsSb-InAs double heterostructure laser operating at 3.2 μm at 78K [13]. The technology for III-V alloy lasers is moderately mature, and we don't expect large improvements in device performance soon.

AUGER RECOMBINATION

Auger recombination in semiconductors (Figure 1) is a nonradiative process which increases rapidly with increasing temperature and emission wavelength. It is believed to be the most important loss mechanism for inter-band MID-IR diode lasers. The temperature and band gap dependence for Auger processes are a result of energy and momentum conservation rules that require participation of electrons (holes) that are above (below) the k=0 point of the energy band. Electrons and holes are distributed in a band of energies within about kT of k=0, and for small band gap semiconductors, electrons and holes may be closer to k=0 and still satisfy the conservation rules.

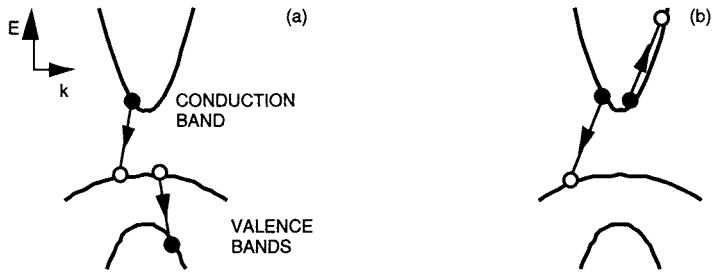

Figure 1. (a) Hole-hole Auger recombination and (b) electron-electron Auger recombination.

TYPE-II SUPERLATTICES

Two semiconductors in contact have a "type-II" band alignment the lowest energy conduction band states and the highest energy valence band states are in different semiconductors as pictured in Figure 2. We call a superlattice type-II if the bulk constituents have a type-II band alignment. If the bulk energy bands line up as in Figure 2a, it is called a staggered alignment superlattice. An example is InAsSb/InAs on a InAs substrate. Spatially indirect recombination occurs with an emission wavelength that can be longer than for the individual constituents. If the valence band in one constituent overlaps the conduction band in another, as illustrated in Figure 2b, it is called a broken gap superlattice. An example is GaInSb/InAs on a GaSb substrate.

Figure 3 provides a more precise description of the GaInSb/InAs broken gap superlattice. The straight solid lines represent bulk energy bands. The dashed lines labeled C1, HH1, and HH2 indicate the lowest energy conduction band state and first and second lowest heavy hole states for the superlattice. Optical transitions are between electrons with wavefunctions (curved lines) weakly localized in the InAs layers and holes with wavefunctions localized in GaInSb.

The energy gap of a type-II superlattice is adjusted by varying the composition of the constituents as well as layer thickness. For the GaInSb/InAs superlattice, the gap is readily adjusted from ~ 3 μm to the far infrared.

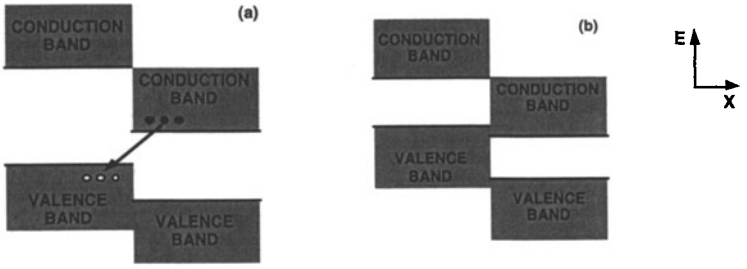

Figure 2. The two kinds of type-II superlattices: (a) staggered alignment and (b) broken gap.

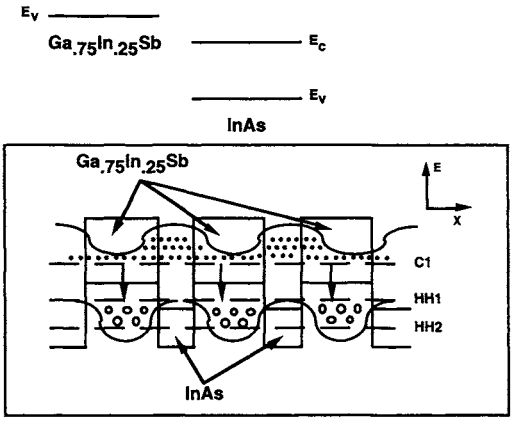

Figure 3. Electron and hole wavefunctions are weakly localized in a GaInSb/InAs superlattice.

Minimizing Auger Recombination

Auger recombination rates for GaInSb/InAs broken gap superlattices can be made small by varying one of the two degrees of freedom - layer thickness and ternary content [8,9]. Choices are subject to the following constraints: i) strain must not be so large as to introduce dislocations, ii) the emission wavelength is specified at the start, and iii) optical transitions must have sufficient oscillator strength for lasing to occur. Relatively thick (35 Å) GaInSb layers keep the growth-axis width of the conduction mini-band less than the energy gap to reduce electron-electron processes. A relatively high In content (25%) in the ternary (to increase the strain splitting of the valence bands) and a judicious choice of superlattice period reduce hole-hole recombination.

Laser Active And Cladding Regions

The type-II superlattice diode lasers discussed here were fabricated at the Hughes Research

Laboratories [14,15]. The active regions were MQW structures with $Ga_{0.75}In_{0.25}Sb$/InAs superlattices for the wells. The most important reason for using MQWs is to reduce the average strain in the active region. GaInSb/InAs superlattices are compressively strained on GaSb, with a critical thickness ~ 1000 Å, but laser active regions must be thicker than 1000 Å for good optical confinement. Unstrained GaInAsSb barriers on either side of the superlattices reduced the average strain, so thicker active layers could be used.

Laser cladding layers are also important for good device performance. AlSb/InAs (25Å/25Å) superlattices were used for the clads. This superlattice has a relatively small refractive index (approximately 3.4 at a wavelength of 3.5 μm) for good optical confinement. The large band gap (approximately 0.85 eV) provides good electrical injection into the active region. The superlattice constituents are oppositely strained with less than 1% lattice mismatch relative to the substrate (Figure 4); thus, thick superlattices with low average strain are readily grown. The growth of the binary constituents requires only a simple calibration procedure. The superlattice also circumvents the difficulties associated with producing n-type material from As-Sb alloys. By doping only the InAs layers, the cladding material was made n-type (8×10^{17} cm^{-3}) using a conventional dopant (Si) for molecular beam epitaxy. Current-voltage measurements on an AlSb(Be)/InAs - AlSb/InAs(Si) pn junction device showed that the junctions were rectifying and had relatively low resistance under forward bias.

More details of the device structure as well as fabrication methods and procedures for device testing can be found in previous publications [14,15].

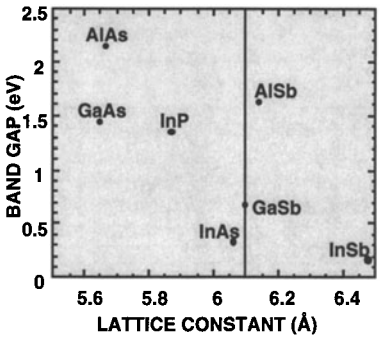

Figure 4. The constituents of an AlSb/InAs superlattice cladding layer are nearly lattice matched to the GaSb substrate.

Laser Performance

Electrically pumped GaInSb/InAs lasers have been demonstrated from 2.8 to 4.3 μm (Figure 5). All devices operated at liquid nitrogen temperature or above. Most of the lasers with a wavelength of 3.4 μm or less operated at temperatures that are accessible by thermoelectric cooling. A 3.2 μm laser operated up to 255 K.

With an 85 μsec current pulse (4.25% duty cycle), a 3.0 μm laser produced 75 mW per facet for the duration of the pulse (Figure 6). The differential quantum efficiency was approximately 4%.

These results are similar to the performance of devices that use the III-V alloys. Perhaps the lack of spectacular results with a type-II superlattice can be explained by differences between the optimized structures proposed by theoreticians (e.g. lasers with infinite superlattice active regions) and those that were actually fabricated. In any case, it is useful to investigate the mechanisms that limited performance.

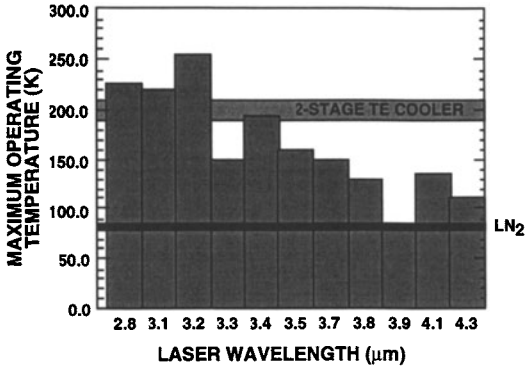

Figure 5. GaInSb/InAs superlattice lasers have been fabricated for a large portion of the mid-infrared.

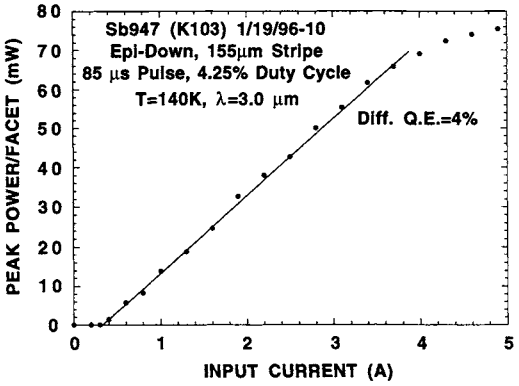

Figure 6. Light versus current for a GaInSb/InAs laser that was approximately 1 mm long.

Prospect For cw Power ≥ 1 Watt

Figure 7 shows calculations for the temperature rise from non-radiative recombination in an active region and from resistive heating in laser cladding layers. The results are for typical lasers with forward bias resistance between 0.5 and 2 ohm. Note that the calculations indicate that resistive heating dominates for all but the smallest input currents. For a 1 ohm laser, we expect an input current of 5 amps to heat the device by 70 K. Given the corresponding decrease in laser efficiency, it is no surprise that we observe saturating output as in Figure 6.

These results suggest that current injection levels should be kept to 5 A or less. Higher currents could be used only with devices that have less resistive cladding layers or heat sinks with higher thermal conductivity (e.g. diamond). To obtain a MID-IR device with cw power equal to or greater than one watt, with a current level of 5 amps, we need at least 20% efficiency. These results also explain why optically pumped lasers, with no resistive heating in the clads, can achieve higher output [16].

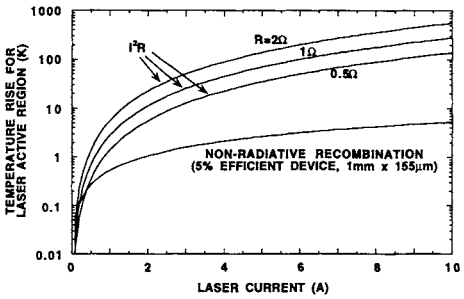

Figure 7. Calculations show that resistive heating is the dominate mechanism for laser heating for all but the smallest input current.

Strain-Balanced Superlattices

Initial calculations for energy bands, wavefunctions, and Auger coefficients were performed for infinite GaInSb/InAs superlattices, but lasers had short, finite length superlattices as described above. Figure 8a shows an unforeseen problem for the finite superlattice. The wavefunction for the high energy HH1 holes is concentrated near the GaInAsSb barriers. There is little overlap between the wavefunctions for the lowest energy electron state C1 and HH1. As a result, we expect a small oscillator strength for this transition and an unfavorable situation - lasing on the C1 to HH3 transition, not the lowest energy transition. Injected holes can occupy HH1 states without contributing to optical gain. The coulomb attraction between electrons and holes, which was not included in these calculations, should mitigate the problem to some extent by increasing the C1-HH1 overlap.

A bigger problem is the difference between the energy bands for the finite and infinite superlattices. The original calculations for Auger recombination rates do not apply to the actual laser active regions. Even worse, the finite superlattice has a very dense valence band structure, so it turns out to be very difficult to tailor the energy bands.

To circumvent these difficulties, a "four layer" superlattice was employed, with the basic period shown in Figure 8b [14]. An AlGaInAsSb layer with tensile strain is used to balance the compressive strain in a GaInSb layer. On average the superlattice is strain free, so it can fill an entire laser active region. The four-layer, strain-balanced superlattice also has a simplified valence band structure which is easier to tailor for reduced Auger recombination.

To date, we have had only limited success fabricating electrically pumped MID-IR lasers using the four-layer superlattice. Optical pumping experiments suggest that the difficulties are related to carrier transport into the active region.

QUANTUM CASCADE LASERS

Recent results with long wavelength, quantum cascade lasers are very impressive [17,18]. Pulsed, single mode, room temperature lasers have been demonstrated at 5.4 and 8 μm. By eliminating valence bands from the lasing process (the "type-I" quantum cascade laser), the quantum cascade design appears to have solved the Auger problem. Another plus is that the quantum cascade lasers use conventional InGaAs and InAlAs layers, lattice matched to InP substrates. On the other hand, the InGaAs/InAlAs conduction band offset limits operation to wavelengths longer than about 4 μm. This is not a fundamental difficulty, and it should be possible to use other semiconductor pairs for shorter wavelength emission.

A more fundamental problem, at least for the first quantum cascade lasers, has been low efficiency. Initially, it appeared that rapid, non-radiative, electron transitions by phonon

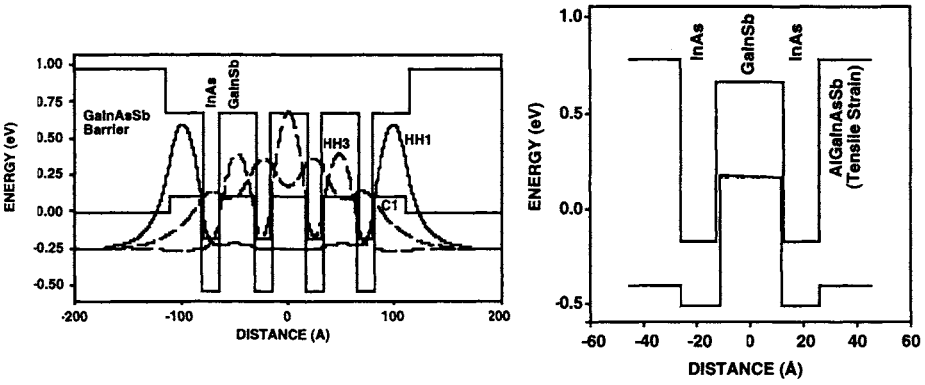

(a) (b)

Figure 8. (a) Calculations predict small wavefunction overlap and weak oscillator strength for the transition from the lowest energy electron state C1 and the highest energy hole state HH1. (b) This four layer superlattice period balances compressive strain in GaInSb with tensile strain in AlGaInAsSb.

emission would make quantum cascade lasers unsuitable for applications that require very high optical power. More recently, dramatic improvements in device efficiency have been reported. A "type-II" (inter-band) quantum cascade laser developed by the University of Houston and the Naval Research Laboratories exhibited an internal efficiency exceeding 100% [19].

ACKNOWLEDGMENTS

I would like to acknowledge Linda West, Tom Hasenberg, Richard Miles, David Chow, Tom Boggess, and Michael Flatté for their work on type-II superlattice lasers. Work on MID-IR lasers at the Hughes Research Laboratories was supported in part by the Air Force Phillips Laboratory under Contract No. F29601-93-C-0037.

REFERENCES

1. R. J. Menna, D. R. Capewell, Ramon U. Martinelli, P. K. York, and R. E. Enstrom, Appl. Phys. Lett. **59**, 2127 (1991).

2. S. R. Kurtz, R. M. Biefeld, L. R. Dawson, K. C. Baucom, and A. J. Howard, Appl. Phys. Lett. **64**, 812 (1994).

3. A. N. Baranov, A. N. Imenkov, V. V. Sherstnev, and Yu. P. Yakovlev, Appl. Phys. Lett. **64**, 2480 (1994).

4. H. Q. Le, G. W. Turner, S. J. Eglash, H. K. Choi, D. A. Coppeta, Appl. Phys. Lett. **64**, 152 (1994).

5. Yong-Hang Zhang, Richard H. Miles, and David H. Chow, IEEE J. Of Selected Topics in Quantum Electron. **1**, 749 (1995).

6. H. K. Choi and G. W. Turner, Appl. Phys. Lett. **67**, 332 (1995).

7. D. H. Chow, R. H. Miles, T. C. Hasenberg, A. R. Kost, Y.-H. Zhang, H. L. Dunlap, and L. West, Appl. Phys. Lett. **67**, 3700 (1995).

8. C. H. Grein, P. M. Young, and H. Ehrenreich, J. Appl. Phys. **76**, 1940 (1994).

9. M. E. Flatté, C. H. Grein, H. Ehrenreich, R. H. Miles, H. Cruz, J. Appl. Phys. **78**, 4552 (1995).

10. Z. Shi, M. Tacke, A. Lambrecht, and H. Böttner, Appl. Phys. Lett. **66**, 2537 (1995).

11. M. Zandian, J. M. Arias, R. Zucca, R. V. Gil, and S. H. Shin, Appl. Phys. Lett. **59**, 1022 (1991).

12. G. W. Turner, M. J. Manfra, H. K. Choi, and M. K. Connors, J. of Crystal Growth, **175/176**, 825 (1997).

13. D. Wu, E. Kaas, J. Diaz, B. Lane, A. Rybaltowski, H. J. Yi, and M. Razeghi, IEEE Photon. Tech. Lett. **9**, 175 (1997).

14. A. R. Kost, L. West, R. H. Miles, T. C. Hasenberg, in *In-Plane Semiconductor Lasers: from Ultraviolet to Midinfrared*, Proc. SPIE **3001**, 321 (1997).

15. T. C. Hasenberg, R. H. Miles, A. R. Kost, and L. West, IEEE J. Quantum Electron. **QE-33**, 1403 (1997).

16. Y. H. Zhang, H. Q. Le, D. H. Chow, and R. H. Miles, in Proc. of the 7th Intl. Conference on Narrow Gap Semiconductors, (IOP, Brystol, 1995) pp. 36-40.

17. Jérome Faist, Federico Capasso, Carlo Sitori, Deborah L. Sivco, James N. Baillargeon, Albert L. Hutchinson, Sung-Nee G. Chu, and Albert Y. Cho, Appl. Phys. Lett. **70**, 2670 (1997).

18. S. Slivken, C. Jelen, A. Rybaltowski, L. Diaz, and M. Razeghi, Appl. Phys. Lett. **71**, 2593 (1997).

19. C. L. Felix, W. W. Bewley, I. Vurgaftman, J. R. Meyer, D. Zhang, C.-H. Lin, R. Q. Yang, and S. S. Pei, IEEE Photon. Technol. Lett. **9**, 1433 (1997).